Acta Crystallographica Section D
Biological Crystallography
ISSN 0907-4449

Crystallization of the *Bacillus thuringiensis* toxin Cry1Ac and its complex with the receptor ligand *N*-acetyl-D-galactosamine

Dean J. Derbyshire,[a]† David J. Ellar[b] and Jade Li[a]*

[a]MRC Laboratory of Molecular Biology, Hills Road, Cambridge CB2 2QH, England, and [b]Biochemistry Department, University of Cambridge, 80 Tennis Court Road, Cambridge CB2 1GA, England

† Present address: Division of Structural Medicine, Wellcome Trust Centre for Molecular Mechanisms of Disease, CIMR, Hills Road, Cambridge CB2 2XY, England.

Correspondence e-mail: jl@mrc-lmb.cam.ac.uk

Received 2 May 2001
Accepted 1 August 2001

Cry1Ac from *Bacillus thuringiensis* ssp. *kurstaki* HD-73 is a pore-forming protein specifically toxic to lepidopteran insect larvae. It binds to the cell-surface receptor aminopeptidase N in *Manduca sexta* midgut *via* the sugar *N*-acetyl-D-galactosamine (GalNAc). By using 1,3-diaminopropane (DAP) as the buffer throughout protoxin activation and chromatography on Q-Sepharose at pH 10.3, trypsin-activated Cry1Ac has been purified in a monomeric state, which was crucial to obtaining single crystals of Cry1Ac and of the Cry1Ac–GalNAc complex. Crystals of Cry1Ac alone are triclinic, with unit-cell parameters $a = 51.78$, $b = 113.23$, $c = 123.41$ Å, $\alpha = 113.11$, $\beta = 91.49$, $\gamma = 100.46^\circ$; those of the Cry1Ac–GalNAc complex show $P2_1$ symmetry, with unit-cell parameters $a = 121.36$, $b = 51.19$, $c = 210.56$ Å, $\beta = 105.75^\circ$. Data sets collected to 2.36 and 2.95 Å resolution, respectively, show that both crystal forms contain four molecules of the 66 kDa toxin in the asymmetric unit and have related packing arrangements. The deaggregating effect of DAP may be explained by its capacity for bivalent hydrogen bonding and hydrophobic interactions at protein interfaces.

1. Introduction

The toxicities of δ-endotoxins produced by *B. thuringiensis* (Bt) during sporulation are specifically directed towards insects of the orders Lepidoptera (moths and butterflies), Diptera (mosquitoes and blackflies) and Coleoptera (beetles) (Höfte & Whiteley, 1989; Margalit, 1989). These toxins recognize receptor proteins on the brush-border membrane surface of the insects' midgut epithelium (Hofmann *et al.*, 1988; van Rie *et al.*, 1989; van Rie, Jansens *et al.*, 1990). Receptor binding triggers a conformational change in the toxin (Li *et al.*, 1991; Schwartz *et al.*, 1997), allowing it to insert into the insect membrane and form lytic pores (Knowles & Ellar, 1987), leading ultimately to insect death (Knowles, 1994). Thus, receptor binding by δ-endotoxins not only determines insecticidal selectivity, but can also affect their pore-forming potency (van Rie, McGaughy *et al.*, 1990; Tabashnik *et al.*, 1994).

Cry1Ac is the only Bt δ-endotoxin, of at least 73 members of the family (Crickmore *et al.*, 1995), for which a membrane receptor and the ligand on that receptor responsible for specificity determination are both known. It is produced by *B. thuriengiensis* ssp. *kurstaki* HD-73 as a protoxin of 133 kDa and proteolytically activated to the 66 kDa toxin (Höfte & Whiteley, 1989) in the midgut of the susceptible insect. The Cry1Ac receptor in the insect *Manduca sexta* has been identified as aminopeptidase N (APN), a 120 kDa glycoprotein with a glycosylphosphatidyl-inositol (GPI) anchor in the membrane (Knight *et al.*, 1994; Garczynski & Adang, 1995; Sangadala *et al.*, 1994). Cry1Ac receptors in several other lepidopteran insects have also been shown to be aminopeptidases N (*e.g.* Gill *et al.*, 1995; Valaitis *et al.*, 1995).

N-acetyl-D-galactosamine (GalNAc) is the high-affinity ligand on *M. sexta* APN specifically recognized by Cry1Ac. It specifically decreased the cytotoxicity of Cry1Ac (Knowles *et al.*, 1984), inhibited the saturable binding of Cry1Ac to BBMV and blocked Cry1Ac binding to the 120 kDa protein in ligand blots (Knowles *et al.*, 1991). In surface plasmon resonance (SPR) experiments using immobilized *M. sexta* APN, GalNAc caused dissociation of bound Cry1Ac with a K_i of 5 m*M*, but not of the closely related Cry1Aa or Cry1Ab which also bind to APN (Masson *et al.*, 1995). SPR analysis of Cry1Ac binding to *M. sexta* APN in a supported lipid monolayer resolved an initial rapid reversible (low-affinity) phase from a slower irreversible (high-affinity) phase (Cooper *et al.*, 1998). Whereas the low-affinity phase was GalNAc-sensitive, the higher affinity phase, which follows first-order kinetics, was sensitive to neither GalNAc nor reagents that disrupt protein–protein interactions. It

suggests that the GalNAc-mediated binding to the APN receptor is immediately followed by a rate-limiting step in the mechanism enabling the toxin to insert into the lipid.

The crystal structure of a Cry1Ac–GalNAc complex will identify directly the toxin residues responsible for recognizing the specificity determinant on insect APN. Comparison of the ligand-bound and free toxin structures can also reveal the immediate structural repercussions of the receptor binding leading to the major conformational change required for pore formation. Clues to specificity determination may also be extracted through structural comparison of Cry1Ac with the closely related Cry1Aa (Grochulski *et al.*, 1995; PDB code 1ciy), which shares a 70% sequence identity with Cry1Ac (Crickmore *et al.*, 1995) but unlike Cry1Ac does not bind GalNAc (Masson *et al.*, 1995), and comparison with the more remotely related Cry3A (Li *et al.*, 1991; PDB code 1dlc), which possesses toxicities to coleopteran rather than lepidopteran insects. We describe here the crystallization of Cry1Ac both as a free toxin and in a complex with GalNAc, with emphasis on overcoming non-specific protein aggregation. Non-crystallographic symmetry in the two crystal forms is also described.

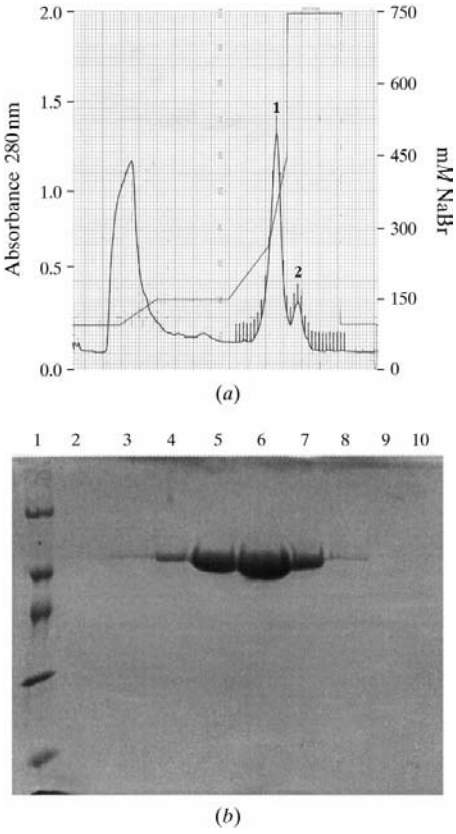

Figure 1
Purification of activated Cry1Ac. (*a*) Elution profile from Q-Sepharose (HiTrap Q) showing absorbance at 280 nm (2 OD full scale) and NaBr concentration in the buffer. (*b*) SDS–PAGE of column fractions through peak 1 (lanes 2–9). Molecular-weight markers (lane 1): 94, 65, 43, 30, 20 kDa.

2. Methods

2.1. Preparation of the Cry1Ac toxin by trypsin cleavage of the protoxin

Parasporal inclusions from *B. thuringiensis* ssp. *kurstaki* HD-73 containing 40 mg of the Cry1Ac protoxin were suspended at 5 mg ml^{-1} in 50 m*M* 1,3-diaminopropane (DAP, Fluka) pH 9.8 containing 300 m*M* NaBr (digestion buffer). A stock solution of *N*-tosyl-L-phenylalanine chloromethyl ketone (TPCK) treated trypsin (Sigma) was brought to 100 mg ml^{-1} in 0.5 m*M* sodium citrate pH 3.0; TPCK (Sigma) was dissolved to 100 m*M* in ethanol. Digestion was initiated by adding 1 mg ml^{-1} of TPCK-treated trypsin and 0.1 m*M* TPCK (final concentrations) to the protoxin suspension. The mixture was incubated in a 310 K water bath with gentle agitation for 10 h. The maximum yield of activated toxin was obtained by collecting the supernatant at 2 h intervals by centrifugation in an Eppendorf microcentrifuge. After adding 0.1 m*M* *N*-tosyl-L-lysine chloromethyl ketone (TLCK, Sigma) and 0.2 m*M* phenylmethylsulfonyl fluoride (PMSF, Sigma) and adjusting the pH to 10.3, the supernatant was immediately subjected to anion-exchange chromatography (see below). The pellet was resuspended in one half of the starting volume in digestion buffer plus 1 mg ml^{-1} TPCK-treated trypsin for continued digestion.

2.2. Anion-exchange chromatography

Pre-packed 5 ml Q-Sepharose anion-exchange columns (Pharmacia HiTrap Q) were connected to a Pharmacia FPLC system. Buffer *A* consists of 34 m*M* DAP pH 10.3; buffer *B* consists of 750 m*M* NaBr in buffer *A*. The column was equilibrated with 25 ml of 13% buffer *B* (98 m*M* NaBr in 34 m*M* DAP pH 10.3). Supernatant from trypsin digestion was adjusted to pH 10.3 by the addition of 0.5 *M* DAP at that pH and loaded onto the column. Trypsin present in this sample was removed by washing the column successively with 50 ml of 13% buffer *B*, 10 ml of a linear gradient of 13–20% buffer *B* (98–150 m*M* NaBr) and 20 ml of 20% buffer *B*. The column was then developed with two consecutive linear gradients of 20–36% buffer *B* (150–270 m*M* NaBr) in 5 ml followed by 36–40% buffer *B* (270–300 m*M* NaBr) in 10 ml. Activated Cry1Ac was eluted in a peak of about 8 ml starting at 28% buffer *B* (210 m*M* NaBr). Finally, the column was washed with 10 ml of 100% buffer *B* and re-equilibrated with 5 ml of 13% buffer *B* for re-use. When the digestion was carried out as successive 2 h incubations, peak fractions containing activated Cry1Ac were pooled from all incubation periods and concentrated by repeating the chromatography procedure as described.

2.3. Protein concentration and pre-mixing of Cry1Ac with GalNAc

For crystallization of the free toxin, activated Cry1Ac was concentrated to 3.5 mg ml^{-1} in 1–2 ml by centrifugal ultrafiltration in Centriprep-30 (Amicon) units spun at 2500 rev min^{-1} at 277 K. It was then dialysed to the starting condition for crystallization at 277 K overnight against a 50 ml reservoir of 50 m*M* DAP pH 10.3 containing 300 m*M* NaBr, 2% 2-methyl-2,5-pentanediol (MPD), 25%(*v*/*v*) glycerol, 3 m*M* NaN_3 and 0.1 m*M* PMSF. The protein concentration increased slightly owing to the osmotic effect of the glycerol and was readjusted to 3.5 mg ml^{-1} by addition of dialysis buffer.

For cocrystallization with GalNAc, ultrafiltration was interrupted when the protein concentration reached 2.5 mg ml^{-1} to allow pre-mixing with the ligand. A 50%(*w*/*v*) solution of GalNAc was prepared in 30 m*M* DAP pH 10.3, 300 m*M* NaBr and 20%(*v*/*v*) glycerol and chilled. 80 µl of the GalNAc stock was added in 10 µl aliquots every 5 min to 2 ml of the Cry1Ac, with gentle mixing by pipette between additions. After the last addition, the mixture was incubated for 1 h on ice before resuming ultrafiltration to a final concentration of ∼3.5 mg ml^{-1}. The sample was dialysed to the starting condition for crystallization, which was identical to that for crystallization of the free toxin except that GalNAc was included at 1.5%(*w*/*v*) and the glycerol concentration was reduced to 20%(*v*/*v*). Protein concentration was readjusted to 3.5 mg ml^{-1}.

2.4. Analytical methods

Protein purity was monitored by SDS–PAGE using Coomassie or silver staining. The N-terminal sequence of major bands was determined after electroblotting onto Immobilon paper. For electrospray mass spectrometry, purified Cry1Ac was dialysed into 0.1%(*v*/*v*) trifluoroacetic acid. Particle-

Table 1
Dynamic light-scattering results fitted to bimodal model.

(*a*) Effects of buffers† used during purification.

Sample					
During activation	During HiTrap Q	D_T‡ ($cm^2\ s^{-1}$)	R_H§ (nm)	% scattering	Est. MW (kDa)
CAPS	CAPS	362	6.8	67	300
		154	16.3	33	3000
CAPS	Piperazine	337	7.3	50	380
		142	17.6	50	3800
CAPS	DAP[a]	469	5.2	14	140
		153	16.3	86	3000
Carbonate	DAP[a]				
		152	16.4	>99	3100
DAP[b]	DAP[a]	9129	0.2	<1	0.15
		647	3.5	>99	60

(*b*) Peaks from HiTrap Q eluted using NaBr.

Sample	D_T‡ ($cm^2\ s^{-1}$)	R_H§ (nm)	% scattering	Est. MW (kDa)
Peak 1	3357	0.77	<1	1.1
	649	3.66	>99	67.4
Peak 2	474	5.0	<15	151
	186	12.9	>85	1410

(*c*) Under starting conditions for crystallization.

Sample	D_T‡ ($cm^2\ s^{-1}$)	R_H§ (nm)	% scattering	Est. MW (kDa)
3.5 mg ml^{-1}, 2% MPD,	537	4.6	10	114
20% glycerol in DAP	359	6.8	90	304

† Buffers: CAPS, 100 m*M* pH 10.5; carbonate, 50 m*M* pH 9.8; DAP[a], 50 m*M* pH 10.3; DAP[b], 20 m*M* pH 9.8; piperazine, 20 m*M* pH 9.8. Where necessary, buffer exchange between activation and ion-exchange chromatography was achieved by gel filtration on a PD-10 column (Pharmacia). ‡ D_T, translational diffusion coefficient. § R_H, mean hydrodynamic radius.

size distribution in solution was determined by dynamic light scattering (D'Arcy, 1994) from Cry1Ac samples at a minimal concentration of 0.5–1.0 mg ml^{-1}, which had been filtered through Milex (MilliPore) syringe filters of 0.02 µm pore size. Measurements were taken on a DynaPro-801 instrument and analysed using the *Dynamics* software supplied by with the instrument. The translational diffusion coefficient (D_T), apparent mass, mean hydrodynamic radius (R_H) and polydispersity (standard deviation of R_H) fitted to a unimodal or bimodal model of size distribution. Goodness of fit was indicated by a baseline close to 1.000 and a sum-of-square error below 1.

2.5. BBMV-binding assay

Brush-border membrane vesicles (BBMV) were prepared from midguts of fifth-instar larvae of *M. sexta* using the Mg^{2+}-precipitation method of Wolfersberger *et al.* (1987) with minor modifications (Carroll & Ellar, 1993). Cry1Ac binding to the BBMV was estimated by the 'spin-down' assay according to Knowles *et al.* (1991). Briefly, BBMV were incubated at 293 K with activated Cry1Ac in phosphate-buffered saline (PBS) containing 1 mg ml^{-1} BSA (to prevent non-specific binding), with or without 2%(*w*/*v*) GalNAc or 20%(*v*/*v*) glycerol or with both, as indicated. After 30 min, the mixture was centrifuged at 12 000*g* for 15 min and aliquots of the supernatant and the pellet (twice washed with PBS) were analysed by SDS–PAGE. A blot of the gel on nitrocellulose paper was incubated with 3%(*w*/*v*) bovine haemoglobin to block non-specific binding, then immune labelled with Cry1Ac-specific antibodies. Bound Cry1Ac antibodies were detected by a reaction using peroxidase-conjugated secondary antibodies.

2.6. Crystallization

Cry1Ac was dialysed in 10 µl microdialysis buttons (Repetition Engineers, Cambridge, England) at room temperature against reservoirs of 2 ml volume held in the wells of 24-well Linbro plates, which were sealed with cover slips and vacuum grease as for hanging drops. This arrangement facilitated screening of different dialysis conditions on a grid. After crystals appeared, the buttons were transferred to 15 ml glass vials to continue dialysis against larger reservoirs at 277 K. The vials were sealed with glass cover slips so that crystal growth could be observed without breaking the seal.

2.7. X-ray data collection and processing

Crystals were stabilized in two stages in buffers containing cryoprotectant. The stabilizing buffer for Cry1Ac crystals consisted of 50 m*M* Tris pH 8.5, 10 m*M* NaBr and 15% glycerol. For cocrystals of Cry1Ac with GalNAc it contained in addition 0.4%(*w*/*v*) GalNAc. Crystals were first transferred to a 1:1 mixture of the final crystallization reservoir and a solution of 50% MPD in the stabilizing buffer, incubated for 10 min and then transferred to a solution of 30% MPD in the stabilizing buffer. Crystals were then flash frozen either by plunging into liquid N_2 or exposing to the N_2 vapour at 100 K.

Diffraction data were collected on MAR image-plate scanners (MAR Research, Hamburg) using a rotating-anode gnerator or synchrotron radiation. Data were processed using *MOSFLM*, *SCALA* and other programs from the *CCP*4 suite (Collaborative Computational Project, Number 4, 1994). Self-rotation functions were calculated using the program *GLRF* (Tong & Rossmann, 1997).

3. Results

3.1. Purity of Cry1Ac

Cry1Ac purified by trypsin activation of the protoxin at pH 9.8 followed by anion-exchange chromatography on Q-Sepharose at pH 10.3 (Fig. 1*a*) showed a single band of about 66 kDa apparent molecular weight on SDS–PAGE (Fig. 1*b*). N-terminal sequencing indicated the first residue to be Ile29, in agreement with the N-terminal activation site reported for other Cry1A toxins (Convents *et al.*, 1991). Electrospray mass spectrometry of the protein dissolved in 0.1%(*v*/*v*) TFA resolved two components present at an abundance ratio of 100:85 with masses of 65 997 and 66 496 Da, respectively. These values correspond closely to the calculated masses, 65 961.1 and 66 473.7 Da, respectively, for two activation products with a common N-terminus at Ile29 and C-termini at Tyr616 and Arg620. Cleavage after Tyr616 shows that some chymotrypsin activity was present during trypsin cleavage of the protoxin, but no detectable chymotrypsin cleavage occurred between Ile29 and Tyr616.

3.2. Aggregation state of purified Cry1Ac

Table 1 presents the results from dynamic light scattering as bimodal size distributions. Monodispersity is normally indicated when >99% of the scattered amplitudes are accounted for by a single size class. Table 1(*a*) shows clearly that with DAP as the buffer during both the activation and anion-exchange steps purified Cry1Ac was monodisperse with a deduced molecular weight of the monomer. In contrast, all other buffers suitable for the required pH range resulted in polydisperse and highly aggregated protein, such that at least one third of the scattering amplitudes were from particles larger than 3000 kDa, roughly 50 times the monomer mass. This clearly indicates non-specific aggregation. Table 1(*b*) and Fig. 1 show that when NaBr was used as the eluting salt, the aggregated material was separated from the monomeric component (peak 1 in Table 1*b* and Fig. 1*a*) into a

Table 2
Lattice constants and data-collection statistics.

Values in parentheses refer to the highest resolution shell.

	Cry1Ac	Cry1Ac–GalNAc
Space group	*P*1	$P2_1$
Unit-cell parameters (Å, °)	*a* = 51.78, *b* = 113.2, c = 123.41, α = 113.11, β = 91.49, γ = 100.46	*a* = 121.36, *b* = 51.19, *c* = 210.56, β = 105.75
Asymmetric unit contents	4 × 66 kDa	4 × 66 kDa
V_M (Å^3 Da^{-1})	2.46	2.38
Thickness of crystal plates (µm)	<25	<15
X-ray source	λ = 1.4 Å, Elettra	λ = 0.87 Å, SRS Daresbury
No. of crystals	3	2
Resolution range (Å)	12–2.36 (2.48–2.36)	40–2.95 (3.11–2.95)
No. of measurements	356898	136564
No. of unique reflections	95726	46735
Completeness (%)	92.4 (88.1)	87.5 (59.7)
R_{merge}† (%)	10.4 (20.2)	13.5 (29.9)
$\langle I\rangle/\sigma(I)$	11.8 (3.9)	8.0 (2.2)

† $R_{merge} = \sum|I - \langle I\rangle|/\sum\langle I\rangle$.

trailing peak (peak 2), whereas when NaCl or KCl was used instead, it barely formed a shoulder on the monomeric peak (data not shown).

After the column-purified monomeric Cry1Ac was dialysed at a protein concentration of 3.5 mg ml^{-1} to the starting condition for crystallizations (§§3.4 and 3.5), dynamic light-scattering measurements (Table 1*c*) indicated formation of particles roughly the size of a tetramer, which accounted for about 90% of the scattering. These particles appear distinct from the larger polydisperse aggregates (Table 1*a*) formed in buffers other than DAP and may represent soluble precursors to the non-crystallographically related pair of dimers observed in the crystals (see §3.7).

3.3. Effect of glycerol on GalNAc-mediated BBMV binding

Glycerol was required at concentrations around 20%(*v*/*v*) in order to change the morphology of Cry1Ac crystals from needles to plates. However, glycerol has been reported to inhibit protein–carbohydrate interaction (Tsitsanou *et al.*, 1999). Therefore, we checked whether GalNAc-mediated receptor binding by Cry1Ac can be maintained in glycerol by comparing Cry1Ac binding to BBMV in the presence and absence of 20%(*v*/*v*) glycerol.

Fig. 2 shows SDS–PAGE analysis of the BBMV-binding assays. In the absence of glycerol, Cry1Ac is entirely bound to the BBMV prepared from midguts of the target insect *M. sexta*, hence it co-sedimented with the vesicles (lanes 8 and 9). Inclusion of 2% GalNAc in the incubation with BBMV completely abolished the binding (lanes 10 and 11), confirming that GalNAc is the high-affinity ligand through which Cry1Ac binds to the membrane receptor in *M. sexta* (Knowles *et al.*, 1991). When 20%(*v*/*v*) glycerol was present in the incubation with BBMV, all except about 5% (judging from intensity of the peroxidase reaction) of the Cry1Ac still co-sedimented with the BBMV (compare lanes 12 and 13 with lanes 8 and 9). When GalNAc was added together with the glycerol, it again completely abolished Cry1Ac binding to BBMV (lanes 14 and 15). Thus, glycerol interference with GalNAc-mediated receptor binding is insignificant and a stable Cry1Ac–GalNAc complex can be observed directly by crystallographic analysis.

3.4. Crystallization of Cry1Ac

In preliminary screens the solubility of Cry1Ac was found to increase with pH, ionic strength and glycerol concentration. By simultaneously reducing all three parameters while increasing the precipitant concentration, nucleation of crystals was induced but the number of nuclei kept to a minimum. Thus, 10 µl of Cry1Ac at the starting conditions (see §2.3) was dialysed at room temperature against 2 ml of 65–69 m*M* piperazine pH 9.8 containing 25–29 m*M* NaBr, 21–25%(*v*/*v*) glycerol, 9% MPD and 1% polyethyleneglycol 350 monomethyl ether. Crystals appeared in 7–10 d. After day 10 the buttons were transferred to 277 K, where crystals were more stable than at room temperature.

Since the starting Cry1Ac concentration could not be made greater than 3.5 mg ml^{-1} without risking uncontrolled nucleation, growth of the crystals soon stopped. Over the next 1–2 months, crystal growth was forced to continue by adjusting the reservoir composition in small increments to decrease protein solubility, while being careful not to trigger secondary nucleation. At intervals of 3–5 d, by diluting the reservoir with appropriate solutions, the MPD concentration was raised by 1–2% each time, NaBr lowered by 1–2 m*M* and glycerol lowered by 0.5%(*v*/*v*). The end point of these adjustments was approximately 15 m*M* NaBr, 15%(*v*/*v*) glycerol and 15%(*v*/*v*) MPD. Concentrations of other reservoir components were kept constant. Crystals of Cry1Ac grew as clusters of thin plates. By these reservoir manipulations, the maximum thickness of the plates was increased from about 10 to 25 µm.

3.5. Crystallization of the Cry1Ac–GalNAc complex

Crystals of the Cry1Ac–GalNAc complex were obtained only through cocrystallization, because crystals of the free toxin dissolved within 2 min of being transferred to a stablization buffer containing as little as 0.1%(*w*/*v*) GalNAc. Once Cry1Ac has been mixed with 2%(*w*/*v*) GalNAc in solution and dialysed against 1.5%(*w*/*v*) GalNAc (§2.3), its solubility is profoundly changed such that even after the Cry1Ac–GalNAc mixture has been extensively dialysed against GalNAc-free buffers, no crystals form under conditions used to crystallize the free toxin. This observation suggests that a specific high-affinity complex between Cry1Ac and GalNAc has formed in solution prior to crystallization, which would be consistent with the ability of GalNAc to displace bound Cry1Ac from BBMV (Knowles *et al.*, 1991; §3.3) or from isolated APN receptors immobilized on the substrate for SPR analysis (Masson *et al.*, 1995). Compared with the K_i of 5 m*M* determined by SPR, the concentration of GalNAc added in solution was at least 13 times greater, so that on average well over 90% of the GalNAc sites on Cry1Ac should be occupied.

Cocrystallization was carried out by dialysing 10 µl of the concentrated Cry1Ac–GalNAc mixture (see §2.3) against 2 ml 68–70 m*M* piperazine pH 9.8 containing 28–30 m*M* NaBr, 20–22% glycerol, 9% MPD and 0.5% GalNAc. Similar results could be obtained when piperazine in the reservoir was substituted with 40 m*M* DAP pH 10.3 and the NaBr concentration reduced to 23–27 m*M* owing to the greater solubility of Cry1Ac in DAP than in piperazine. After equilibrating for 5–7 d during which no crystals appeared, nucleation was induced by lowering the glycerol concentration to 19–20% at the rate of 0.5% per 2 d by adding glycerol-free buffer to the reservoir. By day 15 crystals were visible and the dialysis button was transferred to 277 K. Further growth was forced by slowly reducing glycerol and NaBr concentrations while increasing the MPD concentration in the manner already described for crystallization of the free toxin. Crystals of the Cry1Ac–GalNAc complex also grew as clustered thin

plates; however, they were thinner and more clustered than those of the free toxin. The maximum plate thickness reached was about 15 µm.

3.6. X-ray data collection

Single plates were broken from crystal clusters (Fig. 3), stabilized in cryoprotection buffer and flash-frozen at 100 K. Table 2 shows the data-collection statistics. Using synchrotron radiation, diffraction was observed to a maximum resolution of 1.84 Å from Cry1Ac crystals and to 2.7 Å from Cry1Ac–GalNAc cocrystals. However, owing to radiation sensitivity and non-isomorphism among crystals of the same form (the lattice constants along the shortest axes varied by up to 2 Å), the resolution of the merged data sets was limited to 2.36 Å for the free toxin and 2.95 Å for the complex. Crystals of the free toxin are triclinic; those of the complex show $P2_1$ symmetry. Both crystal forms contained four molecules of the 66 kDa toxin per asymmetric unit.

Lane no.	1	2	3	4	5	6	7	8	9	10	11	12	13	14	15	16	17	18	19
BBMV	-	-	-	-	-	-	+	+	+	+	+	+	+	+	+	-	-	-	-
Cry1Ac	+	+	+	+	-	+	-	+	+	+	+	+	+	+	+	+	+	+	+
GalNAc	-	-	+	+	-	-	-	-	-	+	+	-	-	+	+	-	-	+	+
Glycerol	-	-	-	-	-	-	-	-	-	-	-	+	+	+	+	+	+	+	+
Fraction	S	P	S	P	M			S	P	S	P	S	P	S	P	S	P	S	P

(*a*)

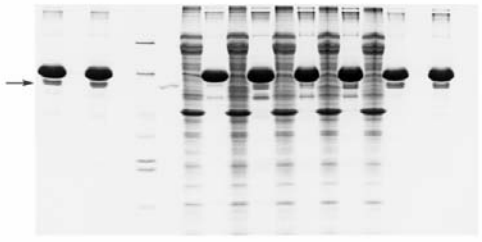

(*b*)

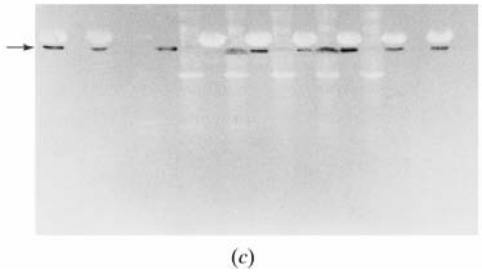

(*c*)

Figure 2
'Spin-down' assay of BBMV binding. Activated Cry1Ac (5 µg) was incubated with *M. sexta* BBMV (equivalent to 2.5 µg of APN), with or without GalNAc [2%(*w*/*v*)], glycerol [20%(*v*/*v*)] or with both, as indicated. The BBMV were spun down and protein contents of the supernatant and pellet analysed by SDS–PAGE. A blot of the gel was immunolabelled with Cry1Ac-specific antibody. Bound specific antibody was then detected by reaction with peroxidase-conjugated secondary antibodies. (*a*) List of the BBMV incubation mixtures from which samples were taken and loaded in each lane. (S, supernatant; P, pellet.) (*b*) Coomassie-stained gel. (*c*) Immunoblot.

3.7. Non-crystallographic symmetry and molecular packing

Self-rotation and self-Patterson maps of the two crystal forms are shown in Figs. 4(*a*) and 4(*b*); their molecular-packing arrangements determined by molecular replacement (Derbyshire and Li, unpublished work) are shown in Figs. 4(*c*) and 4(*d*). For molecular replacement, the coordinates of Cry1Aa (PDB code 1ciy) were used as model for the Cry1Ac-free toxin and refined coordinates of Cry1Ac were then used as model for the Cry1Ac–GalNAc complex. In the *P*1 cell of the free toxin, the four molecules exist as a pair of pairs, one pair shown in red and yellow and the other pair in blue and green (Fig. 4*c*). Within each pair, the molecules are related by a twofold rotation about a non-crystallographic axis nearly parallel to *a* ($\varphi = -0.5$, $\omega = 90$, $\kappa = 180^\circ$), but contact within the pair is not extensive enough for this to be regarded as a dimer. The two pairs are related by a translation vector of fractional coordinates (0.583, 0.012, 0.516). In the $P2_1$ crystal of the Cry1Ac–GalNAc complex, the four molecules in the asymmetric unit are also packed as two pairs. Within each pair the two molecules (red and green or blue and yellow) are related by an approximate twofold rotation about an axis nearest to *a* ($\varphi = 15.9$, $\omega = 99.5$, $\kappa = 168.1^\circ$) and a translation vector nearest to *c* (−0.034, 0.162, 0.484). The red/green pair is related to the blue/yellow pair by a translation vector of fractional coordinates (0.497, 0.450, 0.0). As shown in Fig. 4(*d*), the non-crystallographic symmetry operations combined with the crystallographic 2_1 screw along *b* gives rise to a grouping of four molecules made up by the green and yellow molecules in two adjacent asymmetric units, which has a very similar packing arrangement to the four molecules contained in the *P*1 lattice of the free toxin (Fig. 4*c*).

4. Discussion

4.1. Physiological relevance of Cry1Ac aggregation

The tendency of activated Cry1Ac and other δ-endotoxins to aggregate is well documented. Cry1Ac was reported to aggregate in HEPES at neutral pH in a time-dependent manner (Masson *et al.*, 1995). Time-dependent aggregation of several δ-endotoxins including Cry1Ac at neutral and alkaline pH was detected by size-exclusion chromatography (Guereca & Bravo, 1999), which was thought to reflect the oligomerization anticipated in pore formation under physiological conditions. Our dynamic light-scattering data showed a heterogeneous aggregate size and a dependence of size on the buffer used (Table 1*a*). Therefore, the aggregation *in vitro* cannot be compared directly with oligomerization

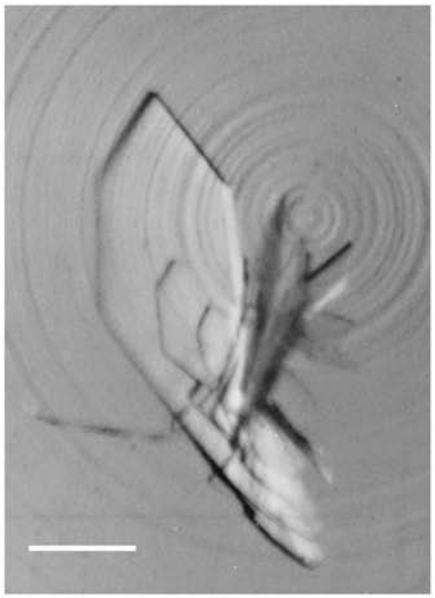

(*a*)

(*b*)

Figure 3
Crystals of Cry1Ac toxin (*a*) and Cry1Ac-GalNAc complex (*b*). Scale bar indicates 250 µm.

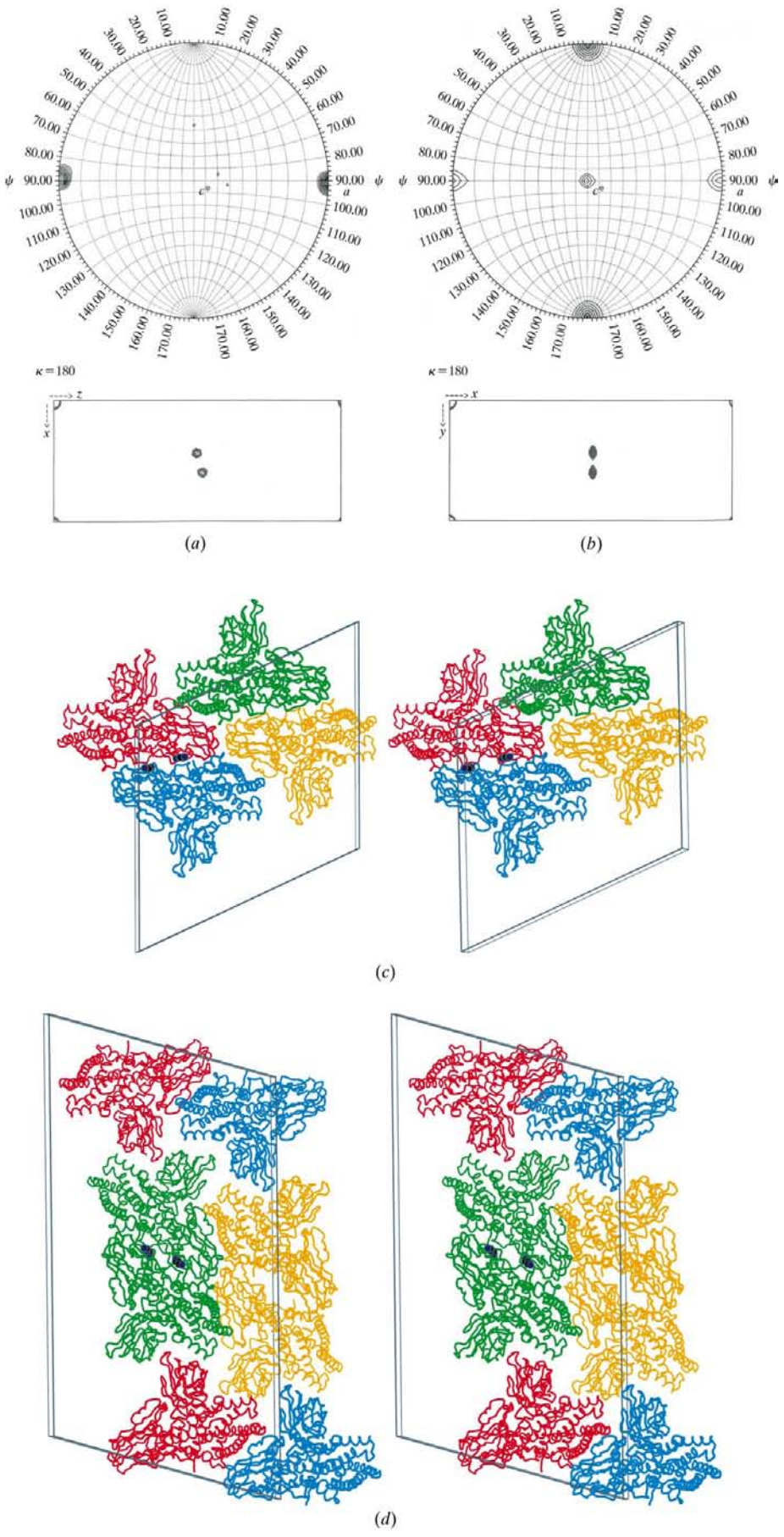

under more physiological conditions (Aronson *et al.*, 1999).

4.2. Diaminopropane as deaggregation agent

Overcoming protein aggregation is critical to success in crystallization. We were able to obtain purified monomeric Cry1Ac only by using the diamine buffer 1,3-diaminopropane (DAP) throughout protein purification. The deaggregating effect of DAP is probably a consequence of its capacity for bivalent hydrogen bonding and hydrophobic interactions. This is supported by details of DAP interaction with Cry1Ac in the structures of the free Cry1Ac and Cry1Ac–GalNAc complex (Derbyshire, Ellar & Li, unpublished work). There is a conserved molecular interface that occurs in the *P*1 crystals of Cry1Ac between the non-crystallographically related red and blue molecules (Fig. 4*c*) and in the $P2_1$ crystals of the complex between two crystallographically related green molecules (Fig. 4*d*). At this interface an ordered DAP molecule has been located in both structures, where its N1 atom is hydrogen bonded to the peptide carbonyl O atom of Asn418 on one protein molecule and its N3 atom is hydrogen bonded to the peptide carbonyl O atom of Asn275 and peptide N atom of Asp277 on the neighbouring molecule, while its C atoms form van der Waals contacts with several non-polar protein side chains from both protein molecules. Since the *P*1 crystals of the free toxin were grown in piperazine buffer rather than DAP and the same $P2_1$ crystals of the Cry1Ac–GalNAc complex can be grown in either DAP or piperazine buffer, the bound DAP molecule must have originated from the purification and become intercalated at the protein interface when purified protein was dialysed against low concentrations of the crystallization reagents MPD and glycerol. Our observa-

Figure 4
Non-crystallographic symmetry (*a*, *b*) and packing arrangement (*c*, *d*) of Cry1Ac molecules in the *P*1 lattice of the free toxin (*a*, *c*) and the $P2_1$ lattice of the Cry1Ac–GalNAc complex (*b*, *d*). The four non-crystallographically related monomers within each asymmetric unit are coloured red, yellow, green and blue. In (*c*), the *P*1 cell of the toxin is viewed along the non-crystallographic twofold which is nearly parallel to *a*, with *b* pointing down and *c* pointing to the upper right. In (*d*) the view is down the crystallographic 2_1 axis along *b*, with *a* pointing to the lower right and *c* pointing up. Note the ordered DAP molecules bound at the conserved molecular interface in both crystal forms.

tion suggests that DAP binding to selected sites on the protein surface can prevent non-specific protein aggreagation and its capacity to bridge two protein molecules can catalyse formation of limited aggregates favourable to ordered crystal growth.

We thank Mr Trevor Sawyer for protoxin preparations, Dr J. G. Carroll for overseeing the modified BBMV-binding assay, Dr Ian Fearnley for mass spectrometry of purified Cry1Ac, Drs J. G. Carroll, R. Henderson and P. R. Evans for helpful comments on the manuscript, and the synchrotron facilities and staff at SRS Daresbury Laboratory and Elettra for support in data collection. This work was supported in part by an MRC Studentship (DJD) and a BBSRC Advanced Research Fellowship (JL).

References

Aronson, A. I., Geng, C.-X. & Wu, L. (1999). *Appl. Environ. Microbiol.* **65**, 2503–2507.

Carroll, J. & Ellar, D. J. (1993). *Eur. J. Biochem.* **214**, 771–778.

Collaborative Computational Project, Number 4 (1994). *Acta Cryst.* D**50**, 760–763.

Convents, D., Cherlet, M., van Damme, J., Lasters, I. & Lauwereys, M. (1991). *Eur. J. Biochem.* **195**, 631–635.

Cooper, M. A., Carroll, J,. Travis, E. R., Williams, D. H. & Ellar, D. J. (1998). *Biochem. J.* **333**, 677–683.

Crickmore, N., Zeigler, D. R., Feitelson, J., Schnepf, E., Van Rie, J., Lereclus, D., Baum, J. & Dean, D. H. (1995). *Microbiol. Mol. Biol. Rev.* **62**, 807–8115.

D'Arcy, A. (1994). *Acta Cryst.* D**50**, 469–471.

Garczynski, S. F. & Adang, M. (1995). *Insect Biochem. Mol. Biol.* **25**, 409–415.

Gill, S. S., Cowles, E. A. & Francis, V. (1995). *J. Biol. Chem.* **270**, 27277–27282.

Grochulski, P., Masson, L., Borisova, S., Pusztai-Carey, M., Schwartz, J.-L., Brousseau, R. & Cygler, M. (1995). *J. Mol. Biol.* **254**, 447–464.

Guereca, L. & Bravo, A. (1999). *Biochim. Biophys. Acta*, **1429**, 342–350.

Hofmann, C., van der Bruggen, H., Höfte, H., van Rie, J., Jansens, S. & van Mellaert, H. (1988). *Proc. Natl Acad. Sci. USA*, **85**, 7844–7848.

Höfte, H. & Whiteley, H. W. (1989). *Microbiol. Rev.* **53**, 242–255.

Knight, P. J. K., Crickmore, C. N. & Ellar, D J. (1994). *Mol. Microbiol.* **11**, 429–436.

Knowles, B. H. (1994). *Adv. Insect Physiol.* **24**, 275–308.

Knowles, B. H. & Ellar, D. J. (1987). *Biochim. Biophys. Acta*, **924**, 509–518.

Knowles, B. H., Knight, P. J. K. & Ellar, D. J. (1991). *Proc. R. Soc. London. Ser. B*, **245**, 31–35.

Knowles, B. H., Thomas, W. E. & Ellar, D. J. (1984). *FEBS Lett.* **168**,197–202.

Li, J., Carroll, J. & Ellar, D. J. (1991). *Nature (London)*, **353**, 815–821.

Margalit, J. (1989). *Isr. J. Entomol.* **23**, 3–8.

Masson, L., Lu, Y.-J., Mazza, A., Brousseau, R. & Adang, M. J. (1995). *J. Biol. Chem.* **270**, 20309–20315.

Rie, J. van, Jansens, S., Höfte, H., Degheele, D. & van Mellaert, H. (1989). *Eur. J. Biochem.* **186**, 239–247.

Rie, J. van, Jansens, S., Höfte, H., Degheele, D. & van Mellaert, H. (1990). *Appl. Environ. Microbiol.* **56**, 1378–1385.

Rie, J. van, McGaughey, W. H., Johnson, D. E., Barnett, B. D. & van Mellaert, H. (1990). *Science*, **247**, 72–74.

Sangadala, S., Walters, F. S., English, L. H. & Adang, M. J. (1994). *J. Biol. Chem.* **269**, 10088–10092.

Schwartz, J. L., Juteau, M. Gruchulski, P., Cygler, M., Prefontaine, G., Brousseau, R. & Masson, L. (1997). *FEBS Lett.* **410**, 397–402.

Tabashnik, B. E., Finson, N., Groeters, F. R., Moar, W. J., Johnson, M. W., Luo, K. & Adang, M. J. (1994). *Proc. Natl Acad. Sci. USA*, **91**, 4120–4124.

Tong, L. & Rossmann, M. G. (1997). *Methods Enzymol.* **276**, 783–792.

Tsitsanou, K. E., Oikonomakos, N. G., Zographos, S. E., Skamnaki, V. T., Gregoriou, M., Watson, K. A., Johnson, L. N. & Fleet, G. W. J. (1999). *Protein Sci.* **8**, 741–749.

Valaitis, A. P., Lee, M. K., Rajamohan, F. & Dean, D. H. (1995). *Insect Biochem. Mol. Biol.* **25**, 1143–1151.

Wolfersberger, M., Lüthy, P., Maurer, A., Parenti, P., Sacchi, F. V., Giordana, B. & Hanozet, G. M. (1987). *Comp. Biochem. Physiol. A*, **86**, 301–308.